Final Report

4GB10, Sustainable fuels: Plan A or B? - Q3 (2024)

Group 03

Full Name	Student ID
Tobias Wejbora	[redacted]

Tutor: Quekel, Daan

Eindhoven, April 2, 2026

Contents

List of symbols

Table 0.1: List of symbols

Symbol	dimension	Unit	Unit abbreviation
V	Volume	Cubic meters	m^3
r	Radius	Meters	m
CC	Displacement volume	Cubic meters	m^3
θ	Crank angle	Radians	rad
U	Voltage	Volts	V
p	Pressure	Pascal	Pa
P	Power	Watts	W
Q	Heat	Joules	J
E	Energy	Kilowatt hours	kWh
η	Efficiency	Dimensionless	[-]
m	Mass	Kilograms	kg
T	Temperature	Kelvin	K
γ	Specific heat	Dimensionless	[-]
c	Specific heat capacity	Joule per Kilogram Kelvin	$JK^{-1}kg^{-1}$
ρ	Density	Kilogram per Cubic Meter	kgm^{-3}
U	Internal energy	Joules	J
A	Area	Meters squared	m^2

1 | Introduction

This project proposes an investigation into the implementation of ethanol as a bio-based fuel in the everyday use of gasoline engines. It has been demonstrated that there is an increasing trend towards the use of bio-based fuels as a possible substitution for fossil fuels, setting global demand for biofuels to grow by 41 billion litres, or 28%, over 2021-2026 (IEA, 2021)[1]. The European Union has put in place regulations regarding bio-based fuels and ethanol blending fuels. Currently, there is a limit to blending certain biofuels due to incompatibility issues with engine parts and parameters. In diesel, the content of bio-diesel, or FAME (Fatty Acid Methyl Ester) is generally limited to 7%. In petrol, the content of ethanol is limited to 10% [2].

The project's overall objective is to provide results on the effects of ethanol-blended gasoline, regarding its efficiency against everyday gasoline. This objective is useful for evaluating biofuels and their possible implementation in the near future. Through the use of numerical modelling and experimentation tools, the team aims towards this main goal. Key engine performance measures will be obtained and extracted through experimentation and modelling of a preliminary and advanced model. The comparison of these models shows a clear contrast between the degree of accuracy obtained through modelling and the results obtained through experimentation.

To fulfill the main objective a clear overall research question has been proposed by the team:
To what extent are the following ethanol-blended fuels: E0, E5, E10, & E15, more efficient and sustainable fuels than pure gasoline in a GX200 engine?

This research question englobes the investigation and purpose of the project, in such a way that the team had a very specific and achievable aim. Within this global research question, several sub-research questions were proposed as branches within this same project, allowing in this manner to provide more measurable, realistic, and timely, points of investigation towards the development of the project.

- In what way do the results of a mathematical model compare to experimentation results for the cycles of a GX200 engine?
- To what extent is a mathematical model accurate in the projection of fuel efficiency for biobased fuels containing larger ratios of ethanol-blended gasoline such as E30 and E40?
- To what extent are ethanol-blended fuels more sustainable within the CO_2 emissions throughout their lifecycle and combustion process than fuels containing less biobased fuel?

Throughout this project, the team has conducted research, experiments, and modelling of ethanol-blended gasoline in an engine to attempt to answer the proposed research question. Two experiments have been carried out for different purposes that will be discussed in more detail further in the report. These experiments were carried out to provide validation of the model and provide more realistic values to the modelling, where a certain amount of dimensions used in the modelling were measured from the disassembling of the engine itself. Another experiment was conducted to obtain values for the pressure and torque of the engine under the use of different fuel compositions and loads. These experiments were key for the understanding of the functioning of the engine and the application of real input to the project.

Furthermore, a MATLAB model is presented in the report. This model attempts to reproduce the efficiency of a gasoline engine with an ethanol-blended fuel. A simple model is presented as a start for the functioning of the engine, and then a more advanced model is designed to decrease the number of assumptions considered in the calculations and to give a more realistic output.

Lastly, this project aims to take a look into biofuels, therefore research on biofuels and corn-based ethanol was conducted. It is key to understand the impact gasoline engines have on the environment and their role in global warming. Therefore a comparison regarding the life cycle of the gasoline engines and the corn-based ethanol was carried out. This provided a more informed and theoretically sustained conclusion on the adaptation of biobased fuels.

2 | Experimentation

An experimentation process was key for the project's development since it gave a real-life perspective to the team's computer modelling. An initial experiment was conducted at the very beginning of the project, consisting mainly of taking measurements and familiarization with the engine model. A second experiment was conducted halfway through the project. This second experiment aimed to measure the pressure and torque of the engine for different fuels such as gasoline or ethanol and gasoline blends to later compare with the results of the model.

2.1 | Experiment 1: Measuring engine dimensions

2.1.1 | Experimental setup

The main goal of the first experiment was to measure specific parameters of the engine that are required to model the engine kinematics. This not only allowed the team to understand the disassembling process of the engine but also had an indirect effect where the group was able to familiarize themselves with the engine that was going to be modelled throughout the project. During the experiment, the engine was disassembled to measure the bore, stroke, displacement volume, dead volume, and compression ratio.

2.1.2 | Experiment results

The measurements were carried out and noted to be compared with the values provided in the specifications of the engine. Table 2.1, portrays the measured engine parameters in the left column, and the theoretical values provided by the engine manual in the right column.

	Theoretical $[cm]$	**Measured** $[cm]$
Bore	6.8	6.78
Stroke	5.4	5.44
Displacement Volume / CC	196.1	196.4
Dead Volume	26.1	19.9
Compression Ratio	8.5	10.85

Table 2.1: Measurements

As observed in the table, the measurements carried out for the bore, the stroke, and the displacement volume were in line with the theoretical values. The measurement for the dead volume deviates from the value provided in the engine manual, resulting in a less accurate calculation of the compression ratio. The dead Volume was a difficult parameter to measure in the experiment, due to its complex shape. To model the parameters of the engine as well as possible, it was determined to use the theoretical values for the dead volume/compression ratio in the model. Regarding the remaining parameters, the measured dimensions were implemented in the model. Lastly, Figure A.2 provides the plot of the volume function made using the kinematics of the engine and the measurements done in experiment 1.

2.2 | Experiment 2: Running Engine for different Fuels and Loads

2.2.1 | Experimental setup

The second experiment carried out by the team had as goal to obtain pV diagrams and other relevant data for cycles of the running engine for combinations of different fuel blends and loads applied to the engine. These cycles are then used to draw conclusions on efficiencies and emissions and are used to validate and compare the model results.

To obtain the pressure-volume diagrams, the pressure in the cylinder and the position of the crank angle were measured using a pressure sensor and pulse sensor. A power generator with three different heater settings was connected to the engine, which functioned as the load on the engine. The three different settings are denoted as: Off (H0), half power (H1), and full power (H2). Different fuels were injected into the engine (E0, E5, E10, E15). These different fuel blends were injected into the engine

where, the fuel consumption, power generation, and fuel rate were measured for each heat setting. This led to a total of 12 different combinations of fuel and heater settings (4 fuels x 3 heater settings). The output voltage values from the pressure sensor and pulse sensor were recorded in Meetpaneel further to save the last cycle iterations of the engine. In Figure A.4 and Figure A.3, the experimental setup can be observed.

During the measurement of each fuel type and heat setting combination, the values of the pulse sensor voltage(V) and the pressure sensor voltage(V) were recorded over time. This was done twice at the point when combustion had ended. These were used to analyze the engine performance for each combination of fuel and heater settings.

After each combination was measured, the team shut down the engine and again saved the values of the pulse and pressure sensor over time for the last iterations of the engine. This was carried out to define top-dead-center (TDC), which is located at the maximum pressure once the engine is motored without ignition. When the engine is shut off, the engine continues rotating for a few seconds, but no ignition occurs. Naturally, this leads to the same crank angle result for each combination of fuel and heater settings.

2.2.2 | Experiment results

For each combination of fuel and heater settings, the pressure sensor and pulse sensor voltages are thus saved twice (see Figure 2.1 for fuel E0 and heater setting 0), in order to obtain data from a significant amount of cycles to reduce error. This data is all converted to pressure expressed in *bar* and volumes expressed in m^3 over time, so time can be eliminated and pV diagrams can be made.

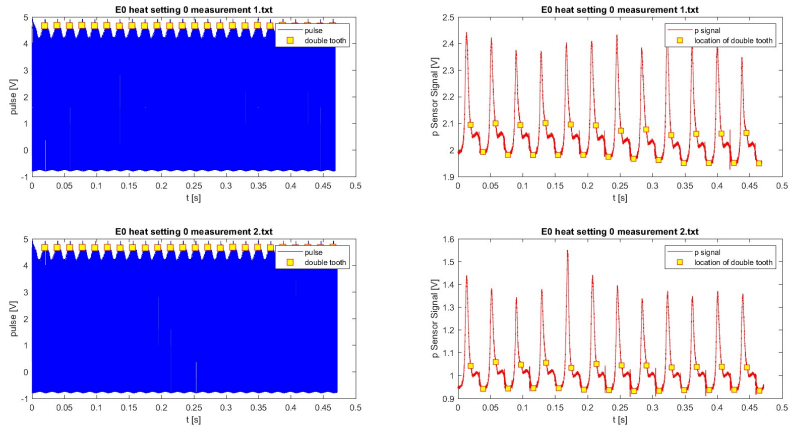

Figure 2.1: Example of the obtained data, fuel E0 and heater setting 0.

Pressure Sensor Validation

The conversion of the pressure voltages to bars was carried out through the following conversion equation:

$$P = \frac{V_{out}}{0.00385 * V_{supply}} - \frac{0.115}{0.00385} \tag{2.1}$$

Where V_{out} is the measured voltage and V_{supply} is the supplied voltage, 5 Volts.

During exhaust, the valve to ambient air is opened and the pressure value remains constant. The offset of the pressure sensor is then corrected by shifting the values of the exhaust stroke to ambient pressure. Setting these pressure values to ambient pressure is therefore a safe way to correct for the pressure sensor offset.

Crank Angle Validation

In order to determine the crank angle over time, which is used to determine the volume over time, the top-dead-centre is determined using the pressure graphs of the validation measurements. As mentioned briefly before, these validation measurements are the measurements done while the engine was shut of, but still motored. No combustion occurs and thus the maximum pressure is a measure of the timing of the top dead center. This way, the crank angle over time is calculated and is therefore converted to volume over time using the kinematics of the engine.

Pressure-volume diagrams Experiments

Using the above validations, the pressure and volume are thus found for all experiment data. The data is structured per cycle and therefore, for each combination of fuel and heater setting, approximately 24 cycles are visualized (saves approximately 12 cycles per measurement, and 2 measurements have been done per combination of fuel type and heater setting). From these experiments, 277 plots of 277 separate cycles have been made in total. The measured output powers from the generator, which are linked to the various heater settings, can be found in Table 2.2.

Throughout the resulting PV diagrams, it can be observed that the peak pressure, intake pressure, and net area of the graphs increase through an increasing load (see Figure 2.2). The cause of this is that more fuel is coming in under the influence of a higher intake pressure to be able to overcome the power out needed for the bigger load. More energy is released during combustion and thus the pressure increases more.

The PV diagrams were used to compare the model results with the experimentation. The experiment plots validated the model parts such as the combustion duration/start and intake pressure for a certain load. Efficiency calculations were carried out with the resulting PV diagrams.

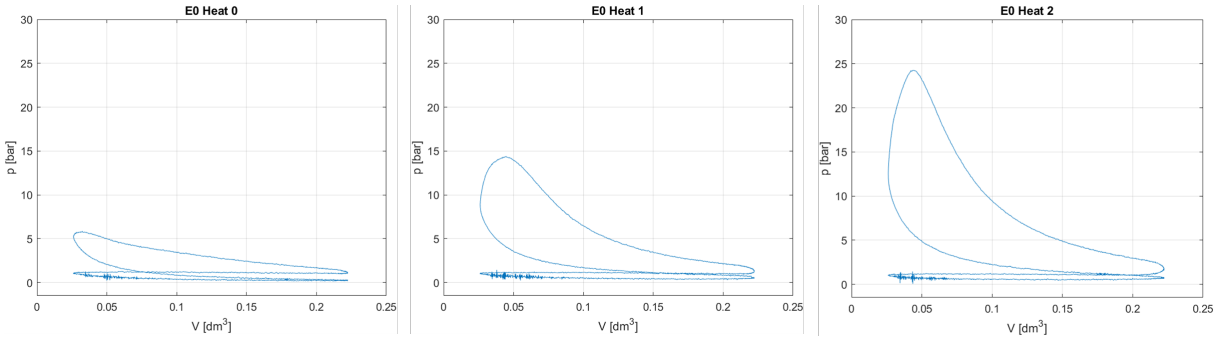

Figure 2.2: Example of experiment result cycles, clear differences between different loads are appreciated.

	Fuel Blends			
Heater Setting	**E0**	**E5**	**E10**	**E15**
0	0	0	0	0
1	996	958	990	996
2	1680	1670	1690	1716

Table 2.2: Output Powers per Heater Setting (W)

Efficiency Results
Using all separate plots for each separate cycle, efficiency calculations are done. The following equation is used to determine the engine efficiency:

$$\eta = \frac{W}{Q_{in}} \tag{2.2}$$

Where W is the work in joules of a single cycle, determined by taking the net area of the cycle using the *trapz* function in Matlab. Q_{in} is the heat supplied by the fuel burned in a single cycle. This value is determined for each cycle using the time in which a certain mass of fuel is burned, which is measured for each combination of fuel type and heater setting. Per combination of fuel type and heater setting, the mean efficiency is determined for all 24 cycles.

Table 2.3 displays the efficiencies of the engine determined through experiment data. Overall, efficiencies are low which is expected due to varying heat loss factors. It is clearly visible that the efficiency increases as both the load and percentage of ethanol increase in the fuel. This is because at higher loads the engine is closer to its ideal operating conditions and thus allows for more complete combustion. Furthermore, Ethanol has a higher RON number of around 109 compared to pure gasoline with an RON number of around 91-93. The higher RON number allows for higher compression ratios without the risk of so-called 'knocking' where combustion does not occur at the most ideal point.

The research octane number (RON) indicates the combustibility of engine fuel at low speeds and temperatures. Since higher compression ratios generally create better fuel combustion, a higher efficiency is expected. Lastly, ethanol tends to run lean due to its higher composition of oxygen, meaning that there is more air in the mixture, leading to more complete combustion and higher efficiencies.

It is important to note the anomaly of the E5 heater setting 0 efficiency. This was the first test run during experimentation meaning that the engine was still relatively cold and therefore more fuel had to be injected into the engine to produce the correct power output. This increase in fuel injection led to a larger efficiency value. Nevertheless, the efficiency results are in line with what is expected.

	Fuel Blends			
Heater Setting	**E0**	**E5**	**E10**	**E15**
0	11.22	12.80	12.05	12.36
1	20.15	20.77	21.38	21.33
2	25.23	26.00	25.93	26.58

Table 2.3: Experiment efficiencies for each Fuel Blend and Load (%)

Further efficiencies were calculated through the experimentation data such as the BSFC. Brake-specific fuel consumption ($g/(kWh)$) is a measure of the fuel efficiency of any engine that burns fuel and produces rotational power output. The BSFC value indicates how efficiently the engine converts fuel supplied into useful work. Table 2.4 provides the given BSFC efficiencies for each fuel blend and heat setting.

	Fuel Blends			
Heater Setting	**E0**	**E5**	**E10**	**E15**
0	800.48	715.56	776.45	747.81
1	414.94	410.73	407.43	417.07
2	331.19	327.53	335.28	333.94

Table 2.4: BSFC Efficiencies [g/kWh]

The literature describes the trend of the use of biofuels in the BSFC as a positive trend where fuels with more ethanol percentage should result in a larger value for the BSFC [3]. This is because ethanol-blended fuels require a large amount of mass to produce the same amount of energy as pure gasoline resulting in a larger value for the BSFC. However, the values obtained in the experimentation do not show a trend of any kind. Although the BSFC calculation is a proper approach to obtaining the efficiency of the fuels, the current table suggests some inaccuracies in the experimentation data regarding its work delivered.

Further analysis was carried out through the experimentation data, where the CO_2 emissions per fuel and heat setting were calculated. As the ethanol part of the fuel does not contribute to the greenhouse effect (elaborated in Section 4), the gasoline-specific CO_2 emissions are most interesting, which can be seen in Table 2.5

	Fuel Blends			
Heater Setting	**E0**	**E5**	**E10**	**E15**
0	2.65E+03	2.24E+03	2.30E+03	2.08E+03
1	1.37E+03	1.29E+03	1.21E+03	1.16E+03
2	1.10E+03	1.03E+03	992	930

Table 2.5: Gasoline specific CO_2 emissions in $[\frac{g}{kWh}]$

A clear trend can be seen in the polluting CO_2 emissions for certain power outputs. Fuel blends with more ethanol are less polluting due to the fact that the CO_2 resulting from the reacting ethanol does not contribute to the greenhouse effect, in contrast with the CO_2 resulting from the reacting gasoline. For higher loads, the engine is more efficient (as can be seen in Table 2.3), and thus less fuel is needed to get a certain power output. Therefore, there also is a decreasing trend in polluting CO_2 emissions in the increasing loads.

3 | Modeling

The team began with an initial simple model, made with the intention to determine the simplest steps of a gasoline engine by the use of assumptions and simplicity, with reference to an ideal Otto cycle. Once this model was defined, a more advanced model started to take shape. It was intended to increase its complexity step by step as assumptions from the simple model were changed into detailed concepts and realistic values.

Combustion Engines follow the Otto cycle. This cycle consists of five different processes: Intake, Compression, Combustion, Expansion, and Exhaust. These five different processes needed to be modelled and connected to provide the required data and plots, and lastly, conclusions could be drawn from these outputs. The main points of interest were the output work, efficiency, and emission, which were key parameters to determine the operational and sustainable performance of the engine.

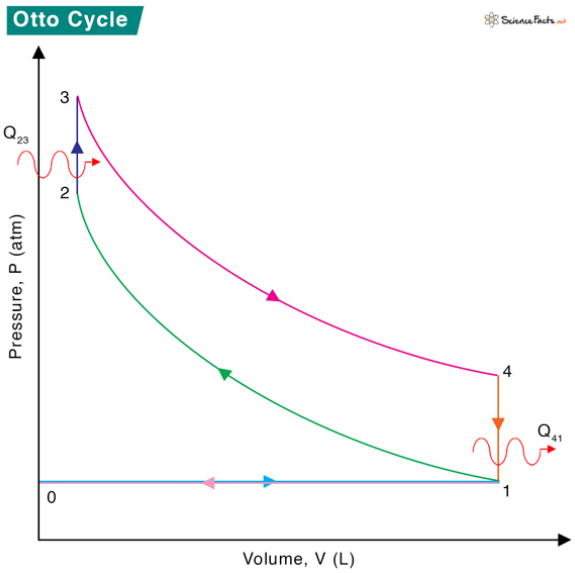

Figure 3.1: Otto Cycle[4]

3.1 | Simple model

The goal of the simple model was to represent the engine's behavior in a thermodynamically ideal world. This meant that a lot of assumptions were made based on an ideal Otto cycle and that all processes within the engine were executed perfectly. Factors such as heat loss and friction were completely neglected for the simple model. The outcomes of this model could therefore be seen as perfectly efficient.

3.1.1 | Initialisation

Before the different functions in the cycle were calculated, the group first needed to obtain the values for all constant parameters of the system. From the experiment, data was retrieved and used for the cycle modelling. Besides this, information on the engine was provided and constants for materials were taken from the internet. Different sources for these values can be found in the references.

The air-fuel ratios are an important value for the efficiency of the model. For the simple model, the assumption was made that in the carburetor, air, and fuel were mixed perfectly according to the stoichiometric air-fuel ratio of the blend. A second assumption was made for the air-fuel ratio. The engine was assumed to run perfectly on this air-fuel ratio. This meant that for the simple model, the value for λ was equal to 1. No surplus of air or fuel would enter the engine.

3.1.2 | Intake

The intake represents the conditions at the very start of the thermodynamic cycle. Pressure and temperature at this point were assumed to be at ambient, *1 bar* and *20 °C* respectively.

For the intake, it was assumed that the volume of the incoming fuel is negligible compared to the volume of the air, $V_{air} >> V_{fuel}$. Besides this, the whole intake phase was assumed to be isothermal and isobaric, meaning that temperature and pressure were considered to be constant. Heat and pressure losses were thus neglected for the ideal model. Finally, the air was assumed to be an ideal gas, therefore using the ideal gas law and the stoichiometric air-fuel ratios, the total mass during the intake phase was calculated.

3.1.3 | Compression and Expansion

For the compression and the expansion, the exact same assumptions were made and the same principles were used to calculate the pressure, temperature, and volume during the process. The first assumption made for these processes was that the processes were adiabatic. Heat losses due to convection were

neglected for the simple model. The volume was calculated according to the volume cycle. Since it was assumed that the process was adiabatic, the pressure and the temperature were calculated using Poisson's relations:

$$pV^{\gamma} = C \tag{3.1}$$

The specific heat(γ) value used in Poisson's relations was set to be equal to the specific heat value for standard day conditions of $\gamma = 1.4$.

3.1.4 | Combustion

For this model, it was assumed that the combustion of the fuel happened instantaneously. Due to the assumption that the air-fuel ratios were stoichiometric, it meant that there were no leftover reactants. It was also assumed that the timing of the combustion was ideal and occurred at the top dead center. Since it was assumed that the combustion was instantaneous, the combustion phase was modeled as isochoric, with the volume of the air-fuel mixture treated as a constant. Since these assumptions are only held for complete combustion and all states just before the combustion are known, the temperatures after the combustion could be calculated using the lower heating value, which is essentially a value representing energy density. The temperatures were then calculated by equation 3.2

$$\Delta T = \frac{1}{AF_{fueltype} + 1} \cdot \frac{Q_{LHV}}{c_v} \tag{3.2}$$

where ΔT is the temperature difference between before and after the combustion and $AF_{fueltype}$, Q_{LHV} and c_v are the fuel-specific air-fuel ratio, lower heating value, and specific volume respectively. Based on these calculated temperatures, the pressures and volumes can be calculated by using the combined gas law.

3.1.5 | Exhaust

The exhaust process completes the cycle. As in the intake phase, the process was assumed to be isothermal and isobaric. Due to the piston rotating, the volume changed. Besides that, the temperature and pressure were set to be equal to an ambient environment.

3.2 | Advanced model

The goal of the advanced model was to represent the behavior of the engine as close to reality as possible. All assumptions made for the simple model were reviewed and where possible, replaced by improved calculations. The advanced model takes into account several notable implementations and changes, such as heat loss, non-instantaneous combustion, and the effects of changing mass fractions.

3.2.1 | Intake

When modeling an engine running on different fuel blends, it will not run on a stoichiometric air-fuel ratio due to the carburetor not being designed for other fuels. The air-fuel ratio changes depending on the density of the fuel and given that $AF_{stoich} = AF$ for gasoline, the following equation can be used to find the area ratio of the carburetor. Using this ratio, the air-fuel ratio can be found for the different fuel blends.

$$AF = AF_{stoich,E0} \cdot \sqrt{\frac{\rho_{air}}{\rho_{fuel}}} \tag{3.3}$$

The respective air-fuel ratios are seen in Table 3.1

Fuel Blend	air-fuel ratio
E0	14,57
E5	14,54
E10	14,52
E15	14,49

Table 3.1: Air-fuel ratios for Various Fuel Blends

Furthermore, the mass of species is initiated in the intake phase. The mass of gasoline and ethanol is given by the air-fuel ratio and respective fuel blend, while the mass of air species is given by the composition of the atmosphere. The ideal gas law is used to determine the mass of air entering the cylinder, which only holds due to the assumption that $V_{air} >> V_{fuel}$. It is thus assumed that the volume of the fuel coming in is negligible compared to the volume of the air coming in, due to the much higher mass density of the fuel. Then the mass of the fuel entering the cylinder is determined using the air-fuel ratio, as elaborated above.

The intake temperature can still be the ambient temperature. The initial pressure is calculated differently in the advanced model, using the experiment data. This is done to scale the power output of the engine. For each cycle retrieved from the experiments, 277 in total, the mean intake pressure is obtained in Matlab. The relation between this mean intake pressure and the load applied to the generator (i.e. measured in the experiment) can be seen in Figure 3.2. By fitting a curve to the data points per fuel, functions have been obtained that are used to model the intake pressure, dependent on the load applied to the generator.

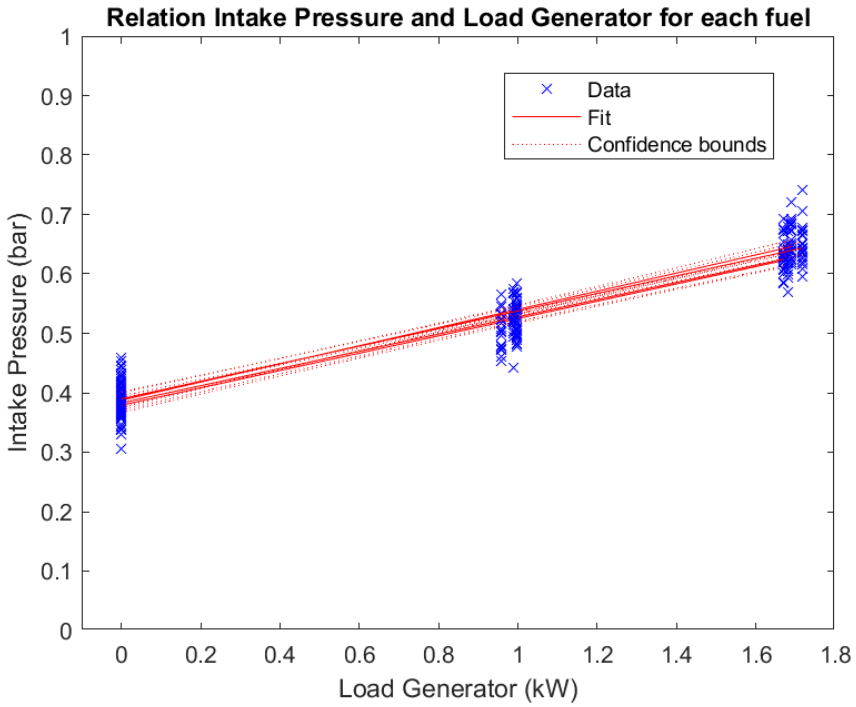

Figure 3.2: Mean Intake Pressure as a function of the load applied to the generator for each fuel blend in the experiment.

The linear relations between the load applied to the generator and the intake pressure are retrieved from the curve fit and manually put in the model for all fuel types, using if statements. This intake pressure is used in the intake part of the model. For the fuel types higher than E15, averages of the linear regression factors resulting for E0, E5, E10, and E15 are used.

3.2.2 | Compression

In the advanced model, it was assumed that the mass of the gas mixture in the engine remains constant. By applying the first law of thermodynamics to a closed system, expressed as $dU = dQ - pdV$, the temperature difference between two successive steps was calculated using the following equation:

$$dT = \frac{dQ - p \cdot dV}{c_v \cdot m} \tag{3.4}$$

Where dQ represented the heat loss at each step, which was accounted for in the heat loss file, and the value of c_v was calculated for each iteration based on the current mass fractions, temperature and NASA tables.

The temperature difference was utilized to determine the new temperature via the equation $T(i) = T(i-1) + dT$. Once the temperature was calculated and the volume of the gas mixture was defined, the pressure of the mixture could be determined using the ideal gas law:

$$p = \frac{m \cdot R \cdot T}{V} \tag{3.5}$$

As can be seen in Appendix B in the main file of the advanced model, at the set moment during compression, combustion starts running simultaneously for a certain crank angle. Then the mass fractions Y and the gas constant R do change. These are both updated in the combustion file and then used for the compression for each next for-loop iteration in the model.

3.2.3 | Combustion

In the advanced model, combustion was not instantaneous and was modelled as a function of the crank angle. By using the Wiebe function to model the amount of fuel burned over the crank angle, the amount of heat created during combustion, and thus the temperature change at each crank angle could be determined. By comparing the model results with the experimental data, it was determined that the angles for the start and duration of combustion, θ_s & θ_d, were 350° and 75° respectively. These values were determined by comparing the shape of the resulting model plots with the experiment plots. Furthermore, coefficients a and n were 5 and 3 as denoted by the project manual. In Equation 3.6, the Wiebe function can be seen. x_b is the fraction of the total amount of fuel that is combusted at a certain crank angle.

$$x_b(\theta) = 1 - exp(-a \cdot (\frac{\theta - \theta_s}{\theta_d})^n) \tag{3.6}$$

The amount of heat released at a certain crank angle can then be calculated using the following equation:

$$\frac{\delta Q_{comb}}{d\theta} = Q_{LHV} \cdot m_{fuel} \cdot n \cdot a \cdot \frac{(1 - x_b)}{\theta_d} \cdot (\frac{\theta - \theta_s}{\theta_d})^{(n-1)} \tag{3.7}$$

Where Q_{LHV} is the lower heating value of the fuel and m_{fuel} the total mass of fuel present at the beginning of combustion/ending of intake.

Using the heat released, the change of temperature dT can be determined using Equation 3.8.

$$dT = \frac{Q_{comb} - p \cdot dV}{c_v \cdot m}; \tag{3.8}$$

In Equation 3.8, Q_{comb} and c_v depend on the mass fractions during combustion and thus need further elaboration. It is known that during combustion, reactants were turned into products; hence, the mass of fuel decreased and the mass of the gases increased. The foundation for calculating mass fractions during combustion was determined using the Wiebe function since it gives the percentage of fuel converted at a certain crank angle. By determining the mass of reactants and mass of products from the combustion reaction equations,

$$C_8H_{18} + 12.5O_2 -> 8CO_2 + 9H_2O \tag{3.9}$$

$$C_2H_6O + 3O_2 -> 2CO_2 + 3H_2O \tag{3.10}$$

an equation for the updated total mass m_s of species during combustion can be formulated.

$$m_s = m_s - m_{reacting} + m_{created} \tag{3.11}$$

To solve for m_s, the mass of reactants (gasoline and ethanol) at each crank angle during combustion could be determined by multiplying the mass of gasoline and ethanol by the difference in x_b. This value gave the amount of gasoline and ethanol reacted per crank angle. These values could be converted into moles by being divided by their respective molar masses. The mass of products could be calculated with the combustion reaction equations which gave the amounts of CO_2 and H_2O created and the amount of O_2 used.

The mass fractions at each crank angle were then given by:

$$Y = \frac{m_s}{sum(m_s)} \tag{3.12}$$

With the updated mass fractions determined, c_v values during each combustion iteration could be derived using the NASA tables.

The mass fractions also play an important role in the pressure calculations since $R_{combustion}$, the gas constant during combustion, depends on the mole fraction of combustion products. The mole fractions could be expressed as moles divided by total moles, where the number of moles per species was the mass divided by molar masses:

$$n_s = \frac{m_s}{Mi} \tag{3.13}$$

$$X_s = \frac{n_s}{sum(n_s)} \tag{3.14}$$

Then the molar mass of solely the gases and therefore the gas constant could be determined using the mole fractions. Then, the pressure could be determined using the ideal gas law.

$$R_{combustiongasses} = \frac{R_{universal}}{M_{combustiongasses}} \tag{3.15}$$

$$p = \frac{m \cdot R_{combustiongasses} \cdot T}{V}; \tag{3.16}$$

As mentioned before, in Appendix B it can be noted that both the compression file and combustion file, as well as both the expansion file and combustion file, are running simultaneously for certain crank angles. Then for instance the pressure and temperatures resulting from compression are used in combustion and overwritten. Then the pressure and temperature increase due to both compression and combustion are accounted for.

3.2.4 | Expansion

The expansion phase operated in a similar manner to the compression phase, the conditions were equal in both processes. The expansion file again runs simultaneously with the combustion file during the first iterations, dependent on θ_d and θ_s.

3.2.5 | Exhaust

During the exhaust process, it was still assumed that the pressure immediately dropped to p_{amb}, resulting in a short isochoric process, after which the phase continued and the volume changed. The temperature was assumed to be equal to the previous temperature, apart from the heat losses to the walls, which were accounted for in the heat loss file. The final mass of piston contents was calculated based on the gas constants of the combustion gases that were calculated during the combustion phase using the ideal gas law.

$$m = \frac{p \cdot V}{R_{combustiongasses} \cdot T}; \tag{3.17}$$

However, the gasses that remain in the dead volume at ambient pressure after the phase are assumed to have no further effect on the full (nor future) cycle(s).

3.2.6 | Heat Loss

When modelling a non-ideal thermodynamic cycle, prominent heat losses arose due to convection between the gases and the cylinder walls. This heat loss was calculated for all crank angles, except when the valves were open. The change in heat loss over each crank angle was determined using the general equation for convection heat losses.

$$\frac{dQ}{dt} = -h_c \cdot A \cdot (T - T_{engine}) \tag{3.18}$$

The convective heat loss coefficient, h_c, was found with the Woschni method where B was the bore, P was the internal pressure of the engine, w was the velocity of the gas, and T was the temperature.

$$h_c = 10.156 \cdot C_1 \cdot B^{-0.2} \cdot (P/1000)^{0.8} \cdot w^{0.8} \cdot T^{-0.8+C_2} \tag{3.19}$$

The velocity(w) was given by the Woschni relation,

$$w = C_3 \cdot S_p + C_4 \cdot V_d \cdot T_r \cdot \left(\frac{P - P_m}{P_r \cdot V_r}\right) \tag{3.20}$$

where S_p denoted the mean piston speed, which could be calculated as stroke divided by the corresponding operation time. V_d was the displacement volume. P_r, V_r, and T_r were respectively the pressure, volume, and temperature of the in-cylinder gas at the start of compression. Lastly, P_m indicated the motorized pressure at the same crank angle as P. The motored pressure was the pressure inside the cylinder in the absence of combustion. This motorized pressure was calculated using the equations for compression and expansion, as could be seen in the advanced model. The properties of the incoming mixture of air and fuel were used throughout the whole cycle, and adiabatic conditions were assumed.

C_1, C_2, C_3, and C_4 were specific coefficients that depended on the part of the thermodynamic cycle. Table 3.2 displayed the respective values for C_1, C_2, C_3 and C_4.

	C_1	C_2	C_3	C_4
Intake	0.287	0.331	6.18	0
Compression	0.287	0.331	2.28	0
Compression/combustion	0.287	0.331	2.28	3.24E-3
Expansion/combustion	0.181	0.390	2.28	3.24E-3
Expansion	0.181	0.390	2.28	3.24E-3
Exhaust	0.181	0.390	6.18	0

Table 3.2: $C3$ and $C4$ for different parts of the thermodynamic cycle [5]

With all variables known for Equation (3.18), the change in heat could be determined.

In the heat loss calculation, the area of heat loss was calculated based on the assumption that the engine could be treated as a perfect cylinder, where its surface area could be calculated as $SurfaceArea = 2\pi \cdot r^2 + 2\pi \cdot r \cdot h$.

The heat loss constants were described for each process in the cycle using if statements. The obtained heat loss per unit time was then converted to an actual (negative) temperature difference, which was added to the current temperature. The complete heat loss file can be seen in Appendix B.

In the temperature curve over crank angle, which can be seen in Appendix C, the functioning of the heat loss can clearly be seen, with heat being added from cylinder walls to gases below T_{engine} (1120 K) and cylinder walls taking heat from the gases above T_{engine}. The temperature of the engine was determined by running extra cycles for the model and taking the equilibrium value for the engine temperature.

3.3 | Model results

The results obtained from the advanced model showed a more accurate representation of the experimental data. These results would be compared with the experimental data through metrics such as efficiency, emissions, fuel blend, and load performance. Graphs have been provided below to portray the model data, which eased comparison between data. However, some points such as peak pressures required specific values for comparison. Table 3.3 provided the peak pressures of the different fuel blends at different loads.

The increase in pressure at higher loads was expected due to the demands for power in the engine. This demand led to higher compression ratios and combustion pressures, which reflected these higher pressures through increasing loads. The table also showed a small peak pressure increase for the higher ethanol content in the fuel composition. This was due to ethanol's slightly higher compression ratios, resulting in this significantly small increase in peak pressure.

	Fuel Blends			
Heater Setting	**E0**	**E5**	**E10**	**E15**
0	11.42	11.48	11.56	11.57
1	15.73	15.58	16.01	15.88
2	18.69	18.62	19.15	18.99

Table 3.3: Max Pressures [bar] for each load and fuel type

The following graphs exhibit a very noticeable common attribute: right skewing. This skewness represents the unidirectional operation of the engine cycle, where the volume decreases as the pressure increases during the combustion stroke. The increase in peak pressure and overall pressure throughout the cycle as load increases, as explained above, is also evident in all graphs below. The graphs of E5 can be seen below in Figure 3.3 as an example. All other graphs can be seen in Appendix C.

3.3.1 | Plots for different loads example - E5

As mentioned in subsection 3.3, there is an increase in pressure as the load of the engine increases. The comparison between the PV diagram and the log-log PV diagram further illustrates the inverse proportionality between pressure and volume. The negative gradient in the log-log graph demonstrates the inverse relationship mentioned, where the pressure increases as the volume decreases inside the engine.

The addition of ethanol leads to an increase in the pressure of the cycle. For E5, this is not a large difference since the amount of ethanol composing the fuel is not significantly large, however a small increase can be observed. This starts a trend towards larger pressures for higher ethanol composition in the fuel, which can further be seen in Appendix C.

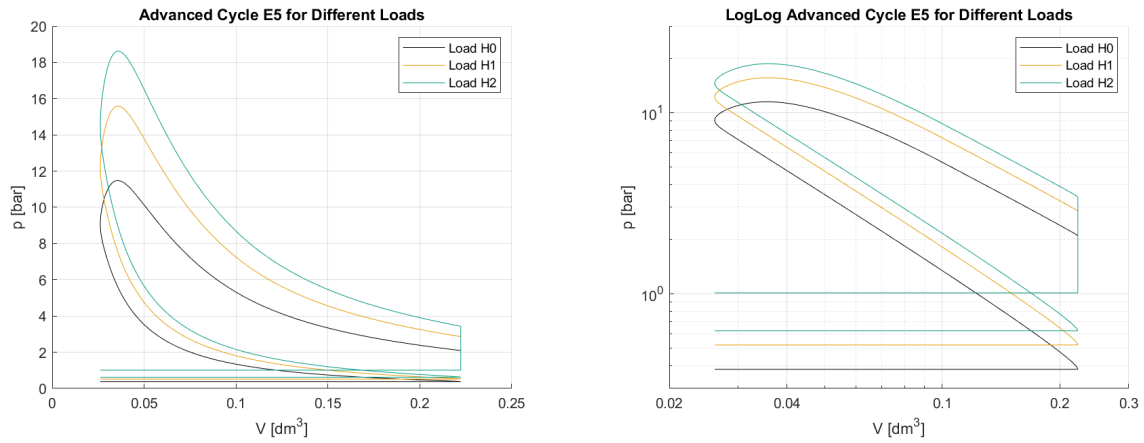

(a) PV Diagram E5 Blend **(b)** LogLog PV Diagram E5 Blend

Figure 3.3: Comparative results for E5 blend

3.3.2 | Efficiencies

The efficiency of an engine depends on multiple variables such as the fuel blend and load. Below are the efficiencies for each tested scenario. The efficiencies of the advanced model for varying fuel blends and loads are seen in Table 3.4. It was chosen to test the same loads as measured per heater setting for each fuel in the experiments, in order to draw clear conclusions on the model's comparison with the experiment.

Efficiencies Model (%)									
Heater Setting	**E0**	**E5**	**E10**	**E15**	**E20**	**E25**	**E30**	**E35**	**E40**
0	31.34	31.95	32.59	33.16	33.51	34.01	34.52	35.01	35.51
1	34.50	35.02	35.85	36.39	36.85	37.42	37.99	38.55	39.12
2	35.84	36.43	37.25	37.82	38.31	38.91	39.50	40.10	40.70

Table 3.4: Model Efficiencies for each combination of Fuel Blend and Load

As observed in the table, for a particular heat setting, the efficiency of the complex model increases as the volume percentage of ethanol increases in each fuel blend. Ethanol, with its higher octane rating compared to gasoline, can lead to higher efficiency. Due to its higher oxygen content, ethanol tends to run lean, resulting in a mixture with more air. This also leads to more complete combustion and higher efficiencies. Besides that, for identical fuel blends, efficiency rises with increasing engine load, as indicated by the heat setting. At higher loads, engines operate closer to their peak efficiency due to factors such as reduced relative heat losses, improved combustion stability, and more efficient utilization of available energy.

3.3.3 | CO_2 Emission Different Fuels Model

The CO_2 emission reflects the sustainability performance of the engine. The CO_2 emissions of the advanced model under different fuel blends and loads are presented in Table 3.5, while the specific CO_2 emissions for gasoline are shown in Table 3.6. These emissions were tested using the same method as the efficiency measurements.

CO_2 Emission Model (g/kWh)									
Load	**E0**	**E5**	**E10**	**E15**	**E20**	**E25**	**E30**	**E35**	**E40**
0	879.92	861.07	842.23	825.56	814.74	800.53	786.69	773.23	760.15
1	799.21	785.68	765.55	752.33	741.01	727.78	714.87	702.27	689.99
2	769.42	755.21	736.75	723.89	712.73	699.90	687.36	675.12	663.17

Table 3.5: Model CO_2 Emissions for each combination of Fuel Blend and Load

For total CO_2 emissions, the amount of CO_2 emitted decreases as the volume fraction of ethanol increases. Similarly, it decreases as the load on the engine increases. Ethanol's oxygen-rich molecular structure results in more complete combustion compared to gasoline, leading to lower CO_2 emissions. Additionally, ethanol's lower carbon content further reduces CO_2 emissions when blended with gasoline.

It's important to note that not all carbon dioxide produced has the same negative impact on the environment, as the ethanol component of the fuel does not contribute to the greenhouse effect, as explained in Section 4.

Gasoline Specific CO_2 Emission Model (g/kWh)									
Load	**E0**	**E5**	**E10**	**E15**	**E20**	**E25**	**E30**	**E35**	**E40**
0	879.92	834.06	788.32	744.69	706.11	664.28	622.52	580.79	539.02
1	799.21	761.03	716.55	678.63	642.21	603.91	565.68	527.49	489.27
2	769.42	731.52	689.60	652.98	617.70	580.77	543.92	507.09	470.25

Table 3.6: Model Gasoline Specific CO_2 Emissions for each combination of Fuel Blend and Load

The same trend is also observed in specific gasoline CO_2 emissions, where the emission decreases with higher ethanol volume fractions and increased engine load. This is because ethanol contains oxygen in its molecular structure. When blended with gasoline, ethanol provides additional oxygen for combustion. This can lead to more complete combustion of both ethanol and gasoline components. This results in

lower CO_2 emissions per unit of gasoline consumed. Furthermore, at higher engine loads, engines tend to operate more efficiently. This improved fuel utilization can result in lower CO_2 emissions per unit of output power.

3.3.4 | Model results analysis

As can be concluded from previously discussed sections, with a higher ethanol volume percentage in the fuel as well as a higher load, the model leads to higher operational efficiency and lower CO_2 emission per output power.

This implies that ethanol, as a biofuel, has certain advantages over conventional fossil fuels when used in internal combustion engines. Therefore, in practical scenarios, using a relatively higher ratio of ethanol in the fuel mixture could lead to higher efficiency and lower CO_2 emissions. Therefore brings sustainable benefits.

3.4 | Experiment and model confrontations

As mentioned in the introduction section, one of the sub-research questions aimed to compare the experiment with the mathematical model. This comparison was crucial for analyzing the accuracy of the modeling. Having an accurate mathematical model allowed for the projection of data for different fuels without the need for experimentation. The experimental process tended to be very precise but was also time-consuming and required significant labor and physical resources.

3.4.1 | PV diagrams confrontations

Figure 3.4 and Figure 3.5 illustrate the comparison between the experimental data and the advanced mathematical model for E10 fuel at different loads corresponding to the heater settings. A trend emerges in the difference between load and pressure peak between the model and the experiment. At low loads, the pressure peak in the model exceeds that in the experimental results, while at high loads, the pressure peak in the experiment surpasses that in the model. For medium load (i.e., heater setting 1), the graphs align well. It can be inferred that the pressure peak of the model exhibits less variation with changing loads compared to what occurs during the experiment. This trend could be attributed to the relationship used for the fuel mass intake in the model, which depends on the intake pressure, not aligning with the actual relationship between the intake pressure and the mass of fuel added in the carburettor. Consequently, the released energy may differ from that in the experiment, leading to a discrepancy in pressure peak. The relationship employed in the model is less sensitive to varying peak pressures than the actual relation in the carburettor.

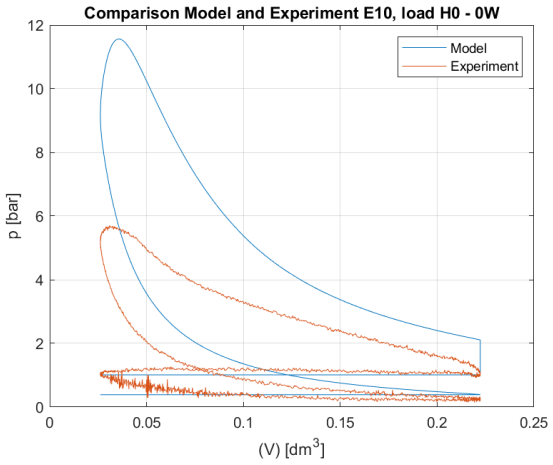

(a) Pressure peak model greater than experiment for low loads.

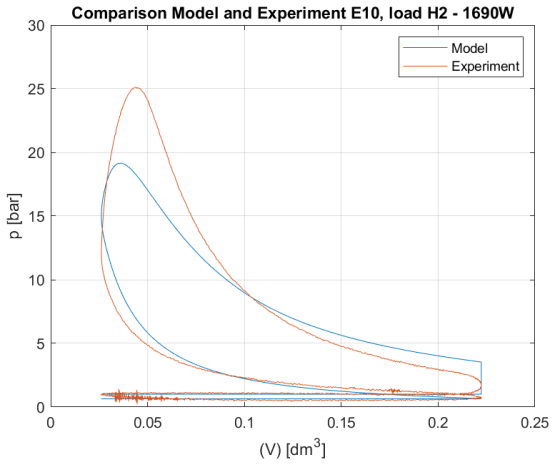

(b) Pressure peak experiment greater than model for high loads.

Figure 3.4: Comparative results for E15 blend

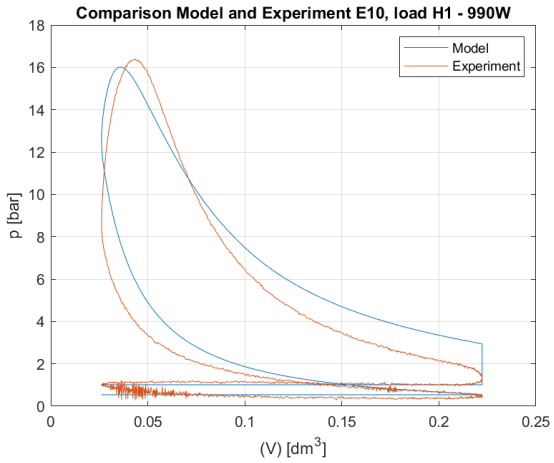

Figure 3.5: Graphs model and experiment align for medium loads, same pressure peak.

3.4.2 | Efficiency and CO_2 Emission confrontations

Despite the less differing mass of fuel intake, which is used to calculate the heat released during combustion for determining efficiency, the efficiencies of the model (Table 3.4) were higher for each fuel and load combination compared to the experiment (Table 2.3). This is caused by the model being more efficient in managing energy losses, including heat losses and neglected friction losses, thereby resulting in higher work output of the engine, which results in higher overall efficiencies. Blow-by was not modeled as well, which also will reduce the efficiencies in the real-world setting.

Furthermore, it can be observed that the model efficiencies differ less per load. This phenomenon is again caused by the less varying incoming mass for varying intake pressures, which is elaborated in subsubsection 3.4.1. With less variation in incoming mass, the work and heat released during combustion exhibit less variation, resulting in efficiencies that are closer to each other across different loads.

Another interesting fact regarding the mass of fuel that came in was the difference in gasoline-specific CO_2 emissions for the model (Table 3.6) and the experiment (Table 2.5). In the experiment, gasoline CO_2 emissions were higher for each load and differed more per load. Here, it can again be concluded that our model was more efficient, requiring significantly less fuel mass to be combusted for a certain work output than in the experiment. Additionally, the differences between loads were smaller for the model, which aligned with the conclusions drawn in subsubsection 3.4.1 regarding the relations used for the incoming mass of fuel concerning the intake pressure.

3.4.3 | Cost Analysis and Fuel Consumption confrontations

A cost analysis and fuel consumption provided financial measurements to help validate the feasibility and implications of the engine.

The cost per hour of running the engine can be determined from the model as seen in Table 3.7. Quantifying the cost per hour of running the engine at a constant rpm allows for the most economical fuel blend and heater setting. Through research, the market has priced ethanol at an average of 0.793 euros per litre [6] and 2.235 euros per litre for E5 gasoline[7]. Note that the price of pure gasoline is hard to obtain through online sources, thus the price of pure gasoline can be determined by Equation (3.21). Furthermore, the cost per hour(CPH) is determined by Equation (3.22), where RPH is rotations per hour.

$$E_{5,price} = G_{price} \cdot Y_g + E_{price} \cdot Y_e \tag{3.21}$$

$$\text{CPH} = (G_{volume} \cdot G_{price} + E_{volume} \cdot E_{price}) \cdot \text{RPH} \tag{3.22}$$

Cost Analysis

The results are seen in Tables 3.7 and 3.8. In general, both the experiment and the model show a decrease in cost as higher ethanol blends are used. This can be linked back to the lower cost of ethanol due to its lower energy density [8]. Furthermore, the price goes up as the load/heater setting is increased. This is clearly due to the fact that more fuel is needed to provide the increase in power output. According to the results of the model, the operational costs ranged from 2.38 euros to 3.62 euros, while the experiment's operational costs ranged from 3.09 euros to 5.73 euros. There was a significant increase in the experiment's operational costs, which was due to factors such as unaccounted-for heat loss factors, i.e., friction, auxiliary, and parasitic losses, not to mention the potential incompatibility of the engine with specific fuel blends.

	Fuel Blends			
Heater Setting	**E0**	**E5**	**E10**	**E15**
0	2.39	2.32	2.26	2.19
1	3.29	3.16	3.15	3.02
2	3.91	3.78	3.77	3.62

Table 3.7: Model: Cost per hour (in euros) of running the engine at 3000rpm

	Fuel Blends			
Heater Setting	**E0**	**E5**	**E10**	**E15**
0	3.09	2.99	2.89	2.79
1	4.75	4.60	4.44	4.29
2	6.36	6.15	5.94	5.73

Table 3.8: Experiment Data: Cost per hour (in euros) of running the engine at 3000rpm

Fuel Consumption

Fuel consumption is another indication of efficiency as it measures the liters of fuel consumed by the engine per hour. For both the model and experimental engine, fuel consumption increased with load and increasing ethanol concentration. This was expected because, as mentioned in the cost analysis, ethanol has a lower energy density, causing more fuel to be injected. Furthermore, the experimental fuel consumption reached higher values for the heater settings, which further indicated that the model didn't account for dynamic processes. These results also went hand in hand with the efficiency calculations, since the experimental engine had lower efficiencies.

	Fuel Blends			
Heater Setting	**E0**	**E5**	**E10**	**E15**
0	1.03	1.04	1.05	1.05
1	1.42	1.41	1.45	1.45
2	1.69	1.69	1.74	1.73

Table 3.9: Model: Fuel consumption (in litres/hour) of the engine at 3000rpm

	Fuel Blends			
Heater Setting	**E0**	**E5**	**E10**	**E15**
0	1.33	1.33	1.34	1.34
1	2.05	2.05	2.05	2.05
2	2.74	2.75	2.75	2.75

Table 3.10: Experiment Data: Fuel consumption(in litres/hour) of the engine at 3000rpm(experiment data)

4 | Green Deal

As introduced at the beginning of the report, sustainable fuels have started to become a common topic in politics as a potential approach to addressing climate change. However, this trend does not yet fully reflect the impact biobased fuels have on the environment, considering their emissions, production, and life cycle.

4.1 | Biobased fuels & Fossil fuels

The main difference between biobased fuels and fossil fuels revolves around the fact of CO_2 emissions. Biobased fuels are produced from plants and living organisms that, during their life cycle, have captured CO_2 for their growth, which is then carried through a chemical process to convert them into fuel. Throughout the combustion of biobased fuels, they emit the CO_2 that they have stored through their life cycle, making this process technically circular in terms of carbon dioxide emission. However, while the process is technically circular, CO_2 emissions are produced through the chemical transformation of the living organisms into biobased fuel. This process emits carbon dioxide, leading to a cycle that is not fully free of CO_2.

This process is very similar to that of the use of fossil fuels. Fossil fuels are extracted from underground reservoirs and then chemically refined into fuel that can be used for consumption. Fossil fuels were also once living organisms and plants that absorbed CO_2, which after millions of years of natural chemical changes, were converted into crude oil. There are two main problems with the use of fossil fuels, one being the limiting amount of these since they take millions of years to produce. The other main issue is regarding its carbon dioxide emissions, a topic that everyone has heard about. Figure 4.1 shows a timeline of the usage of fossil fuels in a timeline starting at the end of the 17th century, prior to the Industrial Revolution.

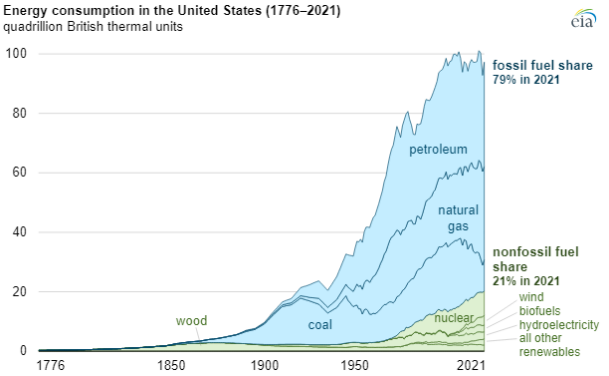

Figure 4.1: Carbon dioxide emissions timeline (EIA, 2022)[9]

The difference between fossil fuels and biobased materials is that millions of plants and living organisms absorbed CO_2 over millions of years and took millions of years to form, and are now all being released in a very short period of time, as has been done during the last 200 years.

4.2 | Sustainability

Against many people's understanding, something that is biobased does not directly mean it is sustainable or CO_2 emissions-free, and biofuels are an example. As briefly mentioned above, the production cycle of biobased fuels is not fully emissions-free. The amount of CO_2 emitted during production, chemical treatment, and transportation varies depending on the crops, location, and treatment. In this project, it is mentioned in the project handbook that the feedstock of ethanol can be disregarded, and hence no specific analysis can be carried out. However, a quick overview of the use of corn ethanol can be analyzed.

According to (G. Cooper, 2022) [10], when all of the emissions tied to making and using gasoline are summed up, the fuel typically has a life cycle carbon intensity of about $98.5 \frac{g}{MJ}$. This is shown in the figure below.

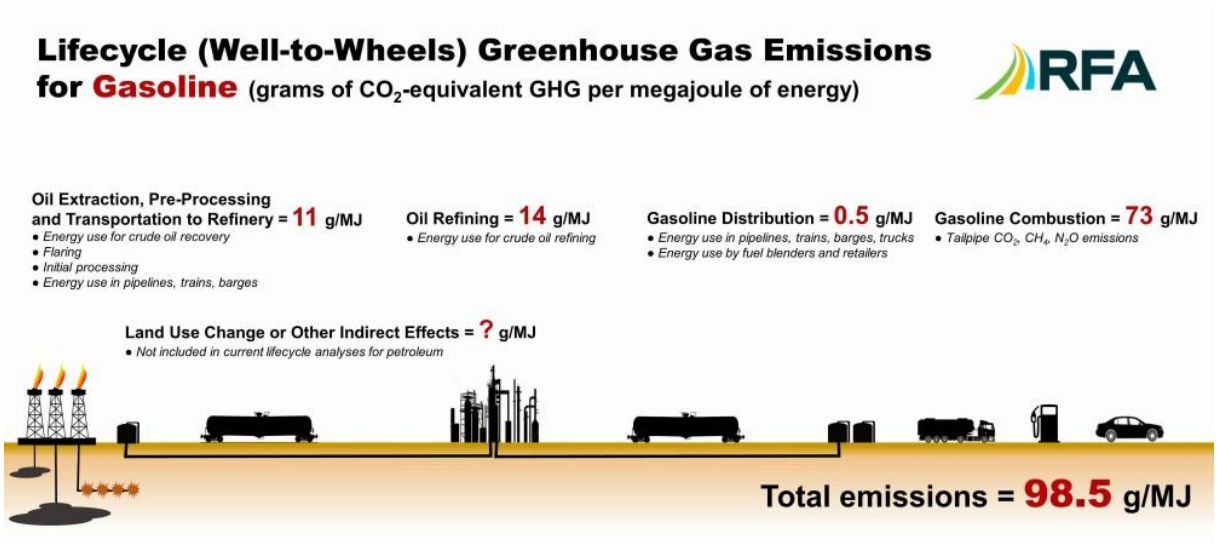

Figure 4.2: Life cycle of gasoline [10]

To put this into perspective, an analysis of the life cycle of corn-based ethanol was carried out. The research states that the life cycle of ethanol production is $53.3 g/MJ$. The following figure provides the life cycle of ethanol production.

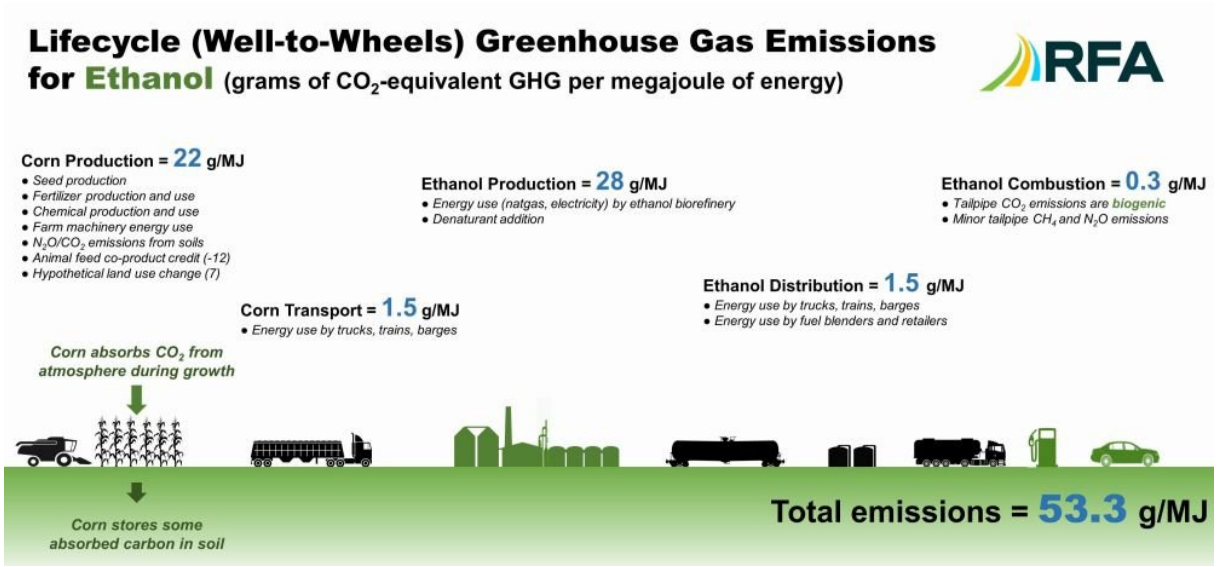

Figure 4.3: Life cycle of ethanol [10]

Comparing both life cycles, it can be appreciated how both the corn production and ethanol production stages, compared to oil extraction and oil refining, produce twice the amount of CO_2 in the ethanol production cycle than in gasoline refining. However, in the end, summing up all stages, the ethanol life cycle is cleaner than the gasoline life cycle, mainly due to the combustion process of gasoline in the engine.

5 | Conclusion

At the beginning of this report, several research questions were presented as part of setting the aim of the project. In this section, these research questions will be answered following the outcomes described in this report.

The first research question formulated was the following:

- In what way do the results of a mathematical model compare to experimentation results for the cycles of a GX200 engine?

The comparison between the model and the experiment can be answered by comparing the results from **Section 2** and **Section 3**. In **Subsection 3.4** the comparison between the experiments and model is further elaborated on.

In conclusion, the model closely mirrors the experimentation results, although the effects that the applied load has on the result can have a substantial impact. Besides that, there are variations in efficiency and CO_2 emissions due to assumptions made to the model and factors such as heat loss, blow by and friction. These assumptions cause the model to have slightly optimistic efficiencies compared to the experiment. These trends can be seen throughout the results for various fuel blends and loads.

Evaluating the second research question:

- To what extent is a mathematical model accurate in the projection of fuel efficiency for biobased fuels containing larger ratios of ethanol-blended gasoline such as E30 and E40?

Using the existing model, efficiency measurements can be projected for fuel blends above 15% ethanol. As previously discussed, the model shows good accuracy compared to that of experimentation, however, the results from the projection of untested fuels are not verified with experimentation. Therefore, unaccounted-for variables/losses might persist. Nevertheless, the projected results showed higher efficiency values and lower CO_2 numbers. At the same time, the fuel economy/cost per hour of these higher fuel blends would also increase due to ethanol's lower energy density. Thus, there is a trade-off with using higher fuel blends as higher costs can deter consumers.

- To what extent are ethanol-blended fuels more sustainable within the CO_2 emissions throughout their lifecycle and combustion process than fuels containing less biobased fuel?

Fuels with a larger bio-ethanol blend are more sustainable than pure gasoline or fuels with a smaller blend. Evidence of this is the lower life-cycle CO_2 emissions. When the lifecycle emissions of gasoline and corn-based ethanol are compared, the sustainable advantage of ethanol arises. Despite the CO_2 emitted during the combustion phase for ethanol, its overall life-cycle emissions are significantly lower than those of gasoline.

Finally, the general research question can be answered.

- **To what extent are the following ethanol-blended fuels: E0, E5, E10, & E15, more efficient and sustainable fuels than pure gasoline in a GX200 engine?**

From the results obtained, it shows that ethanol-blended fuels demonstrate an increase in both efficiency and sustainability over pure gasoline. The report showcases through experimentation and modelling that as the percentage of ethanol in the blend increases, the engine's efficiency improves. This is because of the higher oxygen content of ethanol, causing the combustion to be more complete and leading to higher efficiencies.

Regarding sustainability, ethanol-blended fuels result in a decrease in gasoline-specific CO_2 emissions, so unsustainable CO_2 emissions, per unit of output power. This is in line with the goals for more sustainable fuel usage. Ethanol contributes less to the emissions of greenhouse gases than gasoline does. The lifecycle analysis of corn-based ethanol suggests it is cleaner than gasoline, mainly due to the combustion process in the engine

6 | References

[1] IEA, "Biofuels," *Biofuels – Renewables 2021 – Analysis - IEA*, 2021. [Online]. Available: https://www.eia.gov/todayinenergy/detail.php?id=52959

[2] E. Commission, "Eu action taken on fuel quality," 2022. [Online]. Available: https://climate.ec.europa.eu/eu-action/transport/fuel-quality_en

[3] Ashok, "Investigation on the effect of butanol isomers with gasoline on spark ignition engine characteristics," *Advanced biofuels*, 2019. [Online]. Available: https://www.sciencedirect.com/topics/engineering/brake-specific-fuel-consumption

[4] S. Facts, "Otto cycle," 2022. [Online]. Available: https://www.sciencefacts.net/otto-cycle.html

[5] S. H. Choi, W., "Composition-considered woschni heat transfer correlation: Findings from the analysis of over-expected engine heat losses in a solid oxide fuel celleinternal combustion engine hybrid system," *ScienceDirect*, 2019. [Online]. Available: https://www.sciencedirect.com/science/article/pii/S0360544220309580

[6] A. M. Evelina Lungu, "Viewpoint: Eu ethanol prices likely to rise in 2024," 2024. [Online]. Available: https://www.argusmedia.com/en/news-and-insights/latest-market-news/2522646-viewpoint-eu-ethanol-prices-likely-to-rise-in-2024#:~:text=price%20averaged%20around-,%E2%82%AC793/m%C2%B3,-in%20January%2DSeptember

[7] F. BV, "Price of gasoline within the eu," 2024. [Online]. Available: https://fulltank.nl/en/fuel-prices/

[8] A. TCP, "Ethanol properties: Iea amf work on ethanol," 2019. [Online]. Available: https://www.iea-amf.org/content/fuel_information/fuel_info_home/ethanol/e10/ethanol_properties

[9] EIA, "Fossil fuel sources accounted for 79 percent of u.s. consumption of primary energy in 2021," *U.S. Energy Information Administration*, July 2022. [Online]. Available: https://www.eia.gov/todayinenergy/detail.php?id=52959

[10] G. Cooper, "The truth about ethanol and carbon emissions," *Renewable Fuels Association*, October 2022. [Online]. Available: https://ethanolrfa.org/media-and-news/category/blog/article/2022/10/the-truth-about-ethanol-and-carbon-emissions

A | Appendix A

Experiment 1

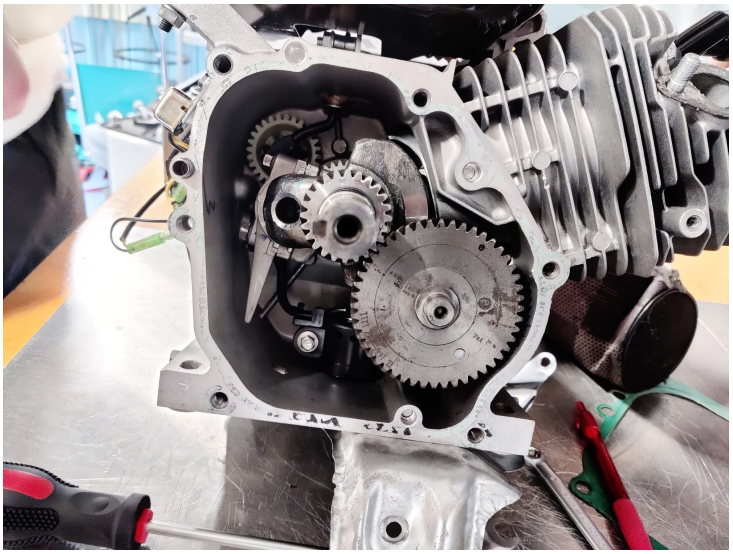

Figure A.1: Experiment 1: Dimensions and timings have been determined.

In Figure A.2, volume calculations using the measurements from the experiment and the valve timing measurements can be seen. This allowed the team to further analyze the efficiency of the measurements carried out in this initial experiment. The graph portrays the changing volume with respect to the crank angle, where several valve timings have been noted.

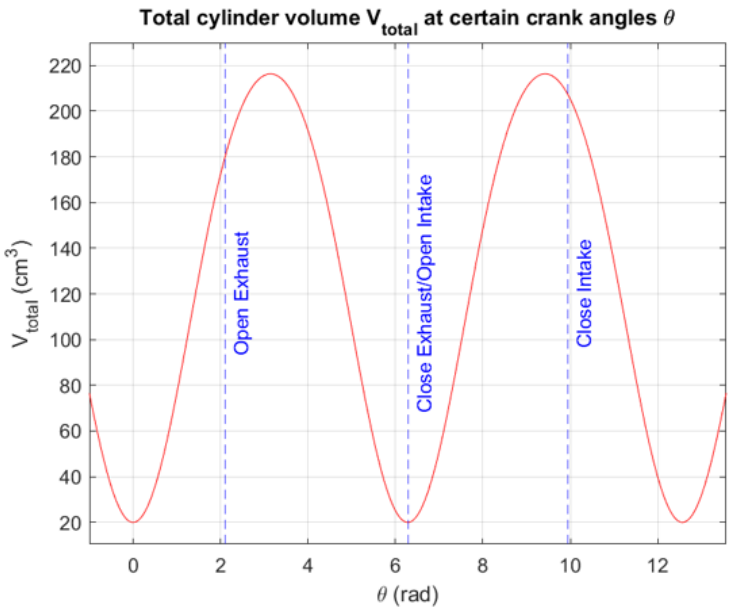

Figure A.2: Volume and Timings with respect to the crank angle.

From this graph, it can be observed that the volume curve is approximately correct, which can be seen in the top dead center volume and bottom dead center volume, which both correspond with the carried-out measurements. Besides, the 4 strokes can clearly be seen during the 2 rotations of the crankshaft, and the top-dead-center volume is again too low as discussed.

Experiment 2

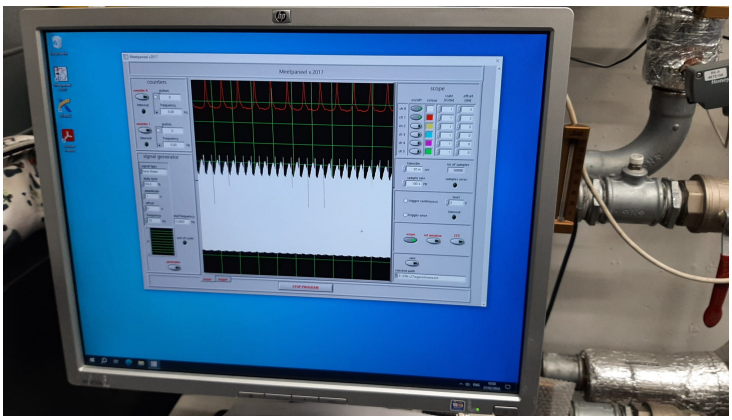

Figure A.3: Experiment 2: Meetpaneel, used to obtain and save the pulse sensor and pressure sensor data.

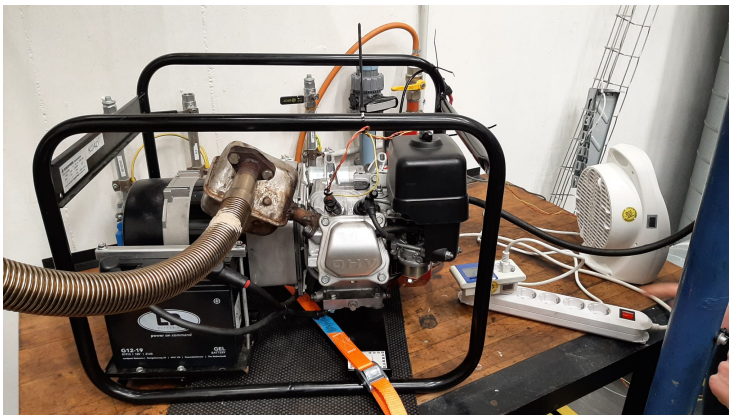

Figure A.4: Experiment 2: Engine, connected to a heater which functions as 3 different loads applied to the generator of the engine.

B | Appendix B

Simple model

```
clear all; close all; clearvars; clc;

NCa =720; % Number of crank - angles
dCa =0.5; % Stepsize
NSteps = NCa / dCa ;

%% Some convenient units
kPa = 1000; kg = 1; mm = 1e-3;


%% Initial conditions / values
S = 54* mm ; % Value info reader
B = 68* mm ; % Value info reader
l = 84.45* mm ; % Our own measurement(not in reader)
rc = 8.5; % Value info reader

NASA_Tables_Setup

% For E0 take AF_s(1), for E5 take AF_s(2) etc.
% For E0 take YfuelE0, for E5 take YfuelE5 etc.
% For E0 take Q_lhv(1), for E5 take Q_lhv(2) etc.
Fuel_Af = AF_s(2);
Fuel_Y = YfuelE5;
Fuel_Q_lhv = Q_lhv(2);

initialization

Ca(1)=0.0;

%% Loop over crank - angle , with 'for ' construction
for i = 2:NSteps
    Ca(i)= Ca(i -1)+ dCa ; % New crank angle for iteration i
    % Intake
    if Ca(i) ≤ 180
        Intake()

    % Compression
    elseif Ca(i) ≤ 360
        Compression()

        % Combustion / Ignition
        if Ca(i) == 360
        Combustion()
        end

    % Expansion
    elseif Ca(i)≤540
        Expansion()

    % Exhaust
    elseif Ca(i)≤720
        Exhaust()
    end
end


figure(1)
plot(V*10^3,p*10^-5)
xlabel('V [dm^3]')
ylabel('p [bar]')
xlim([0 2.4e-1])
ylim([-0.5e1 10.5e1])
title('Ideal Cycle Model E5')
grid on

figure(2)
loglog(V*10^3,p*10^-5)
```

```
xlim([0 2.4e-1])
ylim([0 10.5e1])
xlabel('(V) [dm^3]')
ylabel('p [bar]')
title('LogLog Ideal Cycle Model E5')
grid on


Work_out = polyarea(V,p);
Q_in = mfuel_com * Fuel_Q_lhv;

Efficiency = Work_out/Q_in*100;
disp('Efficiency =');
disp(Efficiency);
```

Listing 1: Main file of the simple model

```
    function V = Vcyl(Ca, S, B, l, rc)
    R = S/2  ;
    Ca = Ca/180*pi;
    Vdisplacement = 1/4 *pi * B^2 *S;
    Vdead = Vdisplacement/(rc-1);
    x = R*cos(Ca)+sqrt(l^2-R^2*(sin(Ca)).^2);
    d = l+R-x;
    V = pi*(B/2)^2*d+Vdead;
end
```

Listing 2: Cylinder Volume function of the model

Advanced model

```
% clear all; clearvars; clc;
debugging = false;
if ¬debugging
    close all
end

NCa =720;            % Number of crank - angles
dCa = 0.5;
NSteps = NCa/dCa;

%% Some convenient units
kPa = 1000; kg = 1; mm = 1e-3;

%% Initial conditions / values
S = 54* mm ;          % Value info reader
B = 68* mm ;          % Value info reader
l = 84.45* mm ;       % Our own measurement(not in reader)
rc = 8.5;             % Value info reader

StartCombustion = 350;
DurationCombustion = 75;

% Fueltype can be adjusted by assigning new string
Fueltype = "E10";                                % E0 to E40 possible (Steps of 5)
load_generator = 1690;                           % Load applied to the generator in watts
                                                 % For instance take load measured in ...
                                                     the experiment (see excel
                                                 % experiment 2 for load for each ...
                                                     combination of fuel and heater
                                                 % setting) to compare model with experiment

NASA_Tables_Setup
initialization

Ca(1)=0.0;

%% Loop over crank - angle , with 'for ' construction
```

```
for i = 2:NSteps
    Ca(i)= Ca(i-1)+ dCa ; % New crank angle for iteration i
    % Intake
    if Ca(i) ≤ 180
        Intake()

    % Compression
    elseif Ca(i) ≤ 360
        Compression()

        % Combustion / Ignition
        if Ca(i) ≥ StartCombustion
        Combustion()
        end

    % Expansion
    elseif Ca(i)≤540
        Expansion()

        % Combustion / Ignition
        if Ca(i) ≤ StartCombustion+DurationCombustion
        Combustion()
        end

    % Exhaust
    elseif Ca(i)≤720
        Exhaust()
    end
        Heatloss()
end

%% plotting
figure(1)
plot(V*10^3,p*10^-5)
xlabel('V [dm^3]')
ylabel('p [bar]')
xlim('auto')
ylim('auto')
title("Advanced Cycle " + Fueltype + ", load " + load_generator + "W")
grid on

% figure(2)
% loglog(V*10^3,p*10^-5)
% xlim('auto')
% ylim('auto')
% xlabel('(V) [dm^3]')
% ylabel('p [bar]')
% title("LogLog Advanced Cycle " + Fueltype + ", load " + load_generator + "W")
% grid on

if debugging
    figure(3)
    plot(diff(p))
    xlim([NSteps/13*6 NSteps/13*7])
end

%% engine performance parameters
Work_out = trapz(V,p);
tolerance = 1e-10;
index_begin_combustion = find(abs(Ca-StartCombustion) < tolerance);
index_end_combustion = find(abs(Ca-(StartCombustion+DurationCombustion)) < tolerance);

mfuel_combusted = m_f(index_begin_combustion)-m_f(index_end_combustion);  % Determine ...
    fuel that is combusted
mgas_combusted = m_s(1,index_begin_combustion)-m_s(1,index_end_combustion);
meth_combusted = m_s(2,index_begin_combustion)-m_s(2,index_end_combustion);
Q_in = mfuel_combusted * Fuel_Q_lhv;

Efficiency = Work_out/Q_in*100;
bsfc = mfuel_combusted/Work_out*3.6e9;% in [g/kWh]
mgasco2_produced = mgas_combusted/Mi(1)*8*Mi(4);
methco2_procuced = meth_combusted/Mi(2)*2*Mi(4);
```

```
107 mco2_produced = mgasco2_produced + methco2_procuced;% mass of co2 produced due to ...
        combustion
108 emmisions_co2 = mco2_produced/Work_out*3.6e9;% in [g/kWh]
109 gas_emissions_co2 = mgasco2_produced / Work_out *3.6e9; % in [g/kWh];
110 eth_emissions_co2 = methco2_procuced / Work_out *3.6e9; % in [g/kWh];
111 disp(['Efficiency = ', num2str(Efficiency), '%']);
112 disp(['Brake Specific Fuel Consumption in [g/kWh] = ', num2str(bsfc)]);
113 disp(['CO2 Emissions in [g/kWh] = ', num2str(emmisions_co2)]);
114 disp(['Ethanol CO2 Emissions in [g/kWh] = ', num2str(eth_emissions_co2)]);
115 disp(['Gasoline CO2 Emissions in [g/kWh] = ', num2str(gas_emissions_co2)]);
116 deviation_work_and_load = ...
        (Work_out-total_load_on_engine_per_cycle)/total_load_on_engine_per_cycle*100;
117 disp(['Deviation work from engine with respect to total load on engine (postive means ...
        Work_out > Total_Load_on_Engine) = ', num2str(deviation_work_and_load), '%   ...
        (ideally 0%)']);
```

Listing 3: Main file of the advanced model

```
1  %Tests if i is defined and if not sets it to 1
2  if exist('i', 'var') ≠ 1
3      i = 1;
4  end
5
6  for j=1:NSp % Compute cp and cv for all species for current temperature
7      Cp(j,i) = CpNasa(T(i-1), SpS(j));
8      Cv(j,i) = CvNasa(T(i-1), SpS(j));
9  end
10
11 cv(i) = Cv(:,i)'*Y(:,i);
12
13 pm(1)=intake_pressure;
14 dV = V(i) - V(i-1);
15
16     if Ca(i) ≤ 180
17         Heat_constant_1 = 0.287;
18         Heat_constant_2 = 0.331;
19         Heat_constant_3 = 6.18;
20         Heat_constant_4 = 0;
21
22         pm(i) = intake_pressure;
23         pm_intake = intake_pressure;
24
25         m_motorized = m(i);
26         T_motorized(i) = T_amb;
27         m_s_motorized = m_s(:,i);
28         Y_motorized = Y(:,i);
29
30
31     elseif Ca(i) ≤ 360
32         Heat_constant_1 = 0.287;
33         Heat_constant_2 = 0.331;
34         Heat_constant_3 = 2.28;
35         Heat_constant_4 = 0;
36         if Ca(i) ≥ StartCombustion
37             Heat_constant_4 = 3.24e-3;
38         end
39
40         for j=1:NSp % Compute cp and cv for all species for current temperature MOTORIZED
41             Cv_motorized(j,i) = CvNasa(T_motorized(i-1), SpS(j));
42         end
43         cv_motorized(i) = Cv_motorized(:,i)'*Y_motorized;
44
45         dT_motorized = (-pm(i-1) * dV) / cv_motorized(i) / m_motorized;
46         T_motorized(i) = T_motorized(i-1) + dT_motorized;
47         pm(i) = sum(m_s_motorized(3:6)) * Rair * T_motorized(i) / V(i);
48
49     elseif Ca(i)≤540
50         Heat_constant_1 = 0.181;
51         Heat_constant_2 = 0.390;
52         Heat_constant_3 = 2.28;
53         Heat_constant_4 = 3.24e-3;
```

```
54
55          for j=1:NSp % Compute cp and cv for all species for current temperature MOTORIZED
56              Cv_motorized(j,i) = CvNasa(T_motorized(i-1), SpS(j));
57          end
58          cv_motorized(i) = Cv_motorized(:,i)'*Y_motorized;
59
60          dT_motorized = (-pm(i-1) * dV) / cv_motorized(i) / m_motorized;
61          T_motorized(i) = T_motorized(i-1) + dT_motorized;
62          pm(i) = sum(m_s_motorized(3:6)) * Rair * T_motorized(i) / V(i);
63
64      elseif Ca(i)≤720
65          Heat_constant_1 = 0.181;
66          Heat_constant_2 = 0.390;
67          Heat_constant_3 = 6.18;
68          Heat_constant_4 = 0;
69          pm(i) = P_amb;
70      end
71
72  velocity = Heat_constant_3 * w_p +  ...
        Heat_constant_4*V_dis_th*T_amb*(p(i)-pm(i))/(intake_pressure*(V_dis_th+V_dead_th));
73  hc(i) = 10.156 * Heat_constant_1 * Bore_th^-0.2 * ((p(i)/1000))^0.8 * velocity^0.8 * ...
        T(i)^(-0.8+Heat_constant_2);
74  dQheat(i) = -hc(i)*Area_heatloss*(T(i)-T_engine)*tCa;
75
76  dT_heatloss(i) = dQheat(i)/cv(i)/m(i);
77  T(i) = T(i) + dT_heatloss(i);
```

Listing 4: Heat loss file of the advanced model

C | Appendix C

Temperature curve, functioning heat loss

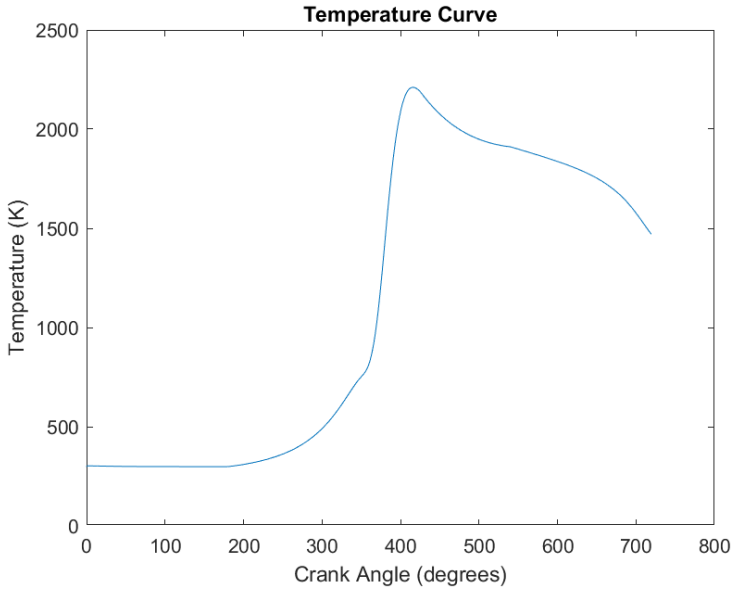

Figure C.1: Temperature Curve, functioning of heat loss can be seen → Adding heat from cylinder walls to gasses below heat_engine (1120 K) and cylinder walls taking heat from the gasses above heat_engine.

Model resulting graphs for different loads - E0, E10, E15

E0

As mentioned in subsection 3.3, there is an increase in pressure as the load of the engine increases. From the comparison between the pV diagram and the log-log pV diagram, the inverse proportionality between pressure and volume mentioned is further represented. The negative gradient in the log-log graph shows the inverse relationship mentioned, where the pressure increases as the volume decreases inside the engine.

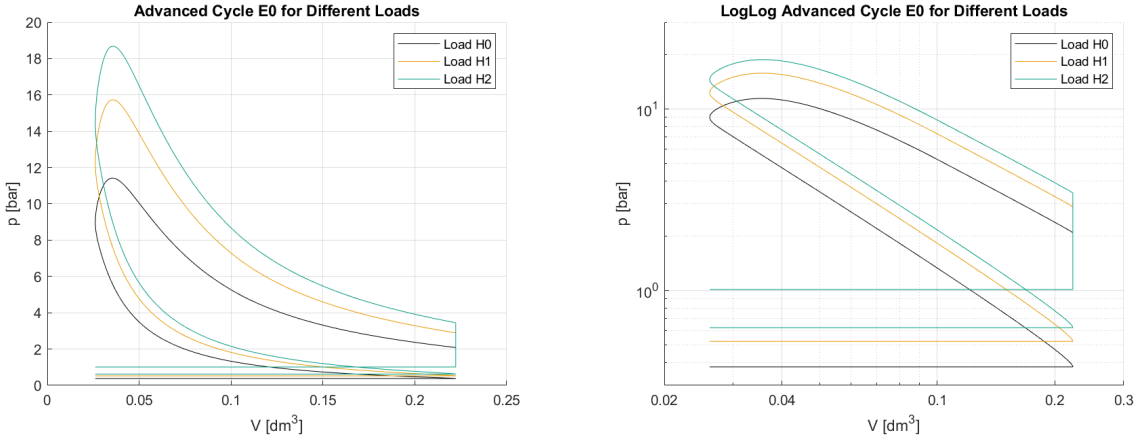

(a) PV Diagram E0 Blend

(b) LogLog PV Diagram E0 Blend

Figure C.2: Comparative results for E0 blend

E10

The pressures for E10 are slightly higher due to the larger intake pressures. Intake pressures are reliant on the experimental data therefore having an impact on the results portrayed in the graphs. The above mentioned trends carry on through the values for this fuel blend.

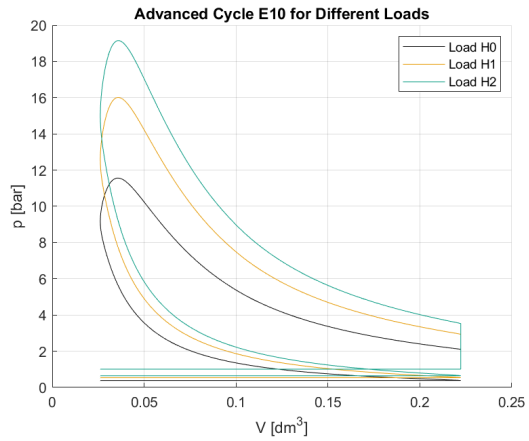

(a) PV Diagram E10 Blend

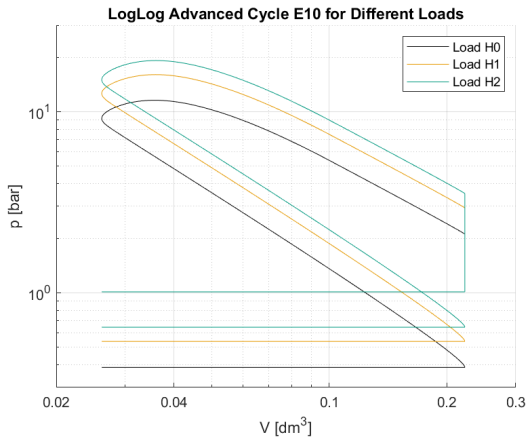

(b) LogLog PV Diagram E10 Blend

Figure C.3: Comparative results for E10 blend

E15

The results for E15 show the largest pressures compared to those of previous fuel blends. This again shows the trend of larger pressure for higher ethanol compositions in the fuel. This trend is shown also for all loads as presented at the beginning.

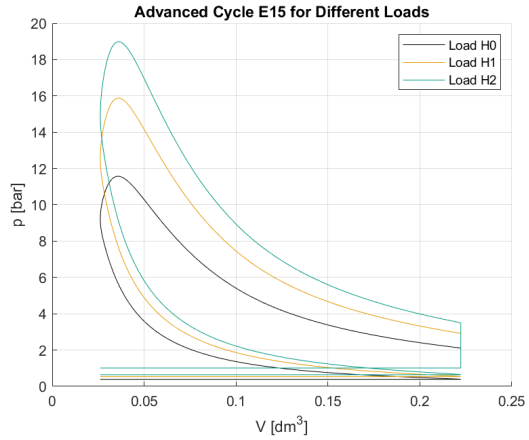

(a) PV Diagram E15 Blend

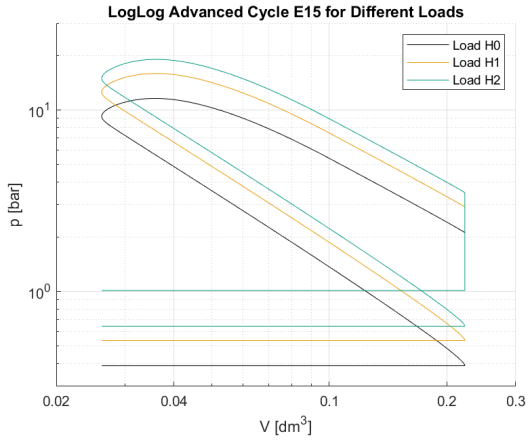

(b) LogLog PV Diagram E15 Blend

Figure C.4: Comparative results for E15 blend